

UNSTEADY WETNESS EFFECTS IN LP STEAM TURBINES

Kane D. Chandler*
 Hopkinson Laboratory
 Department of Engineering
 University of Cambridge
 Cambridge, CB2 1PZ
 United Kingdom
 Email: kdc22@cam.ac.uk

Alexander J. White
 Hopkinson Laboratory
 Department of Engineering
 University of Cambridge
 Cambridge, CB2 1PZ
 United Kingdom
 Email: ajw36@cam.ac.uk

John B. Young
 Hopkinson Laboratory
 Department of Engineering
 University of Cambridge
 Cambridge, CB2 1PZ
 United Kingdom
 Email: jby1@cam.ac.uk

ABSTRACT

One of the unresolved issues for condensing flow in large steam turbines is correct prediction of the droplet size distribution. Optical measurements taken in the later stages of LP steam turbines have shown that the time-averaged droplet size spectra are much broader with larger average diameters than predicted by most theoretical and computational methods. Previous work has suggested that the broad distributions might stem from unsteadiness created by the interaction between successive blade rows – the so-called 'wake-chopping' effect. The current paper presents preliminary results of multi-stage CFD calculations aimed at investigating the impact of such unsteadiness on the condensation process.

A method for calculating unsteady, viscous, condensing flows in multi-stage steam turbines is first outlined. This is based on an established single-phase flow solver with nucleation and droplet growth incorporated via moment evolution equations for the polydispersed liquid phase. The method can be used to compute two- and three-dimensional steady and unsteady flows, time accuracy being preserved for unsteady calculations by means of the dual time-stepping technique. Comparison between computed results and experimental data is presented for nozzle and cascade flows for the purpose of validation. Finally, results are presented for a two-dimensional unsteady multi-stage calculation, highlighting the impact of wake-chopping and related unsteady phenomena on the droplet spectra.

NOMENCLATURE

| | |
|--------------|--|
| e | specific internal energy, [Jkg^{-1}] |
| f | droplet number density function, [$\text{m}^{-1}\text{kg}^{-1}$] |
| G | droplet growth rate, dr/dt , [ms^{-1}] |
| h | specific enthalpy, [Jkg^{-1}] |
| h_{fg} | specific enthalpy of vapourisation, [Jkg^{-1}] |
| J | nucleation rate, [$\text{s}^{-1}\text{kg}^{-1}$] |
| Kn | Knudsen number |
| M | Mach number |
| p | pressure, [Nm^{-2}] |
| Pr | Prandtl number |
| q_c | condensation coefficient |
| r | droplet radius, [m] |
| R | specific gas constant, [$\text{Jkg}^{-1}\text{K}^{-1}$] |
| s | specific entropy, [$\text{Jkg}^{-1}\text{K}^{-1}$] |
| T | temperature, [K] |
| T_d | droplet temperature, [K] |
| \mathbf{u} | velocity vector, [ms^{-1}] |
| y | wetness fraction |
| ΔT | subcooling, [K] |
| λ | vapour thermal conductivity, [$\text{Wm}^{-1}\text{K}^{-1}$] |
| μ_j | j^{th} moment of size distribution |
| ρ | density, [kgm^{-3}] |
| σ | liquid surface tension, [Jm^{-2}] |

subscripts

| | |
|--------|--------------|
| ℓ | liquid water |
| g | gas phase |

*Address all correspondence to this author.

| | |
|-----|-------------------|
| j | moment index |
| s | saturation value |
| 0 | stagnation value |
| * | critical value |
| 32 | Sauter mean value |

Other symbols are defined in the text where they are introduced.

1 INTRODUCTION

Almost a century ago, Baumann proposed a rule of thumb for estimating wetness losses in wet-steam turbines. In the intervening years, engineers have acquired an understanding of how water droplets form and grow in high speed steam flows, but no physical model to predict the wetness losses has been forthcoming. One reason is that it has not been possible to predict the correct size distribution of fog droplets formed in LP turbines. Theory gives acceptable agreement with laboratory nozzle and cascade experiments [1], but predicting the broad range of droplet sizes observed in LP turbines has so far defied theoretical modelling. Obtaining the correct droplet size distribution is a crucial step in the prediction of wetness losses, water deposition onto blade surfaces and other two-phase phenomena since these depend strongly on droplet radii.

One hypothesis is that the broad spectra observed in real turbines stem from unsteady wake-chopping effects. Segmentation of the wakes in successive blade rows means that fluid 'particles' passing through the turbine experience different levels of dissipation, thereby spreading the condensation process over several blade rows. The wake-chopping effect was first analysed by Gyarmathy & Spengler [2] who were concerned with explaining total temperature fluctuations observed in turbine exit flows. They were also aware, however, of the implications for phase change. Later, Bakhtar & Heaton [3] provided an estimation of the effect on droplet sizes by means of a simple statistical model. This involved using a random variable to assign the circumferential location of fluid particles at entry to each blade row, coupled with assumed pitch-wise loss profiles and a simplified (tabulated) condensation model. Their results showed a broadening of droplet spectra as a consequence of the fluctuating dissipation levels, but the precise shape of the size distributions was found to be quite sensitive to the assumed loss profiles. Guha & Young [4] refined the statistical model by employing Lagrangian-style nucleation and droplet growth calculations, tracking large numbers of fluid particles through a flowfield determined by a streamline curvature throughflow calculation. Wake profiles and wake propagation were put on a firmer theoretical footing but nonetheless required a degree of *ad hoc* physical modelling. Predicted droplet spectra were again found to be broadened by the unsteadiness and sometimes showed slight bi-modality, this being in keeping with optical measurements [5].

Using an essentially identical method to that of Guha & Young, Petr & Kolovratnik [6] undertook statistical calculations for a 200 MW LP turbine, comparing their results with optical measurements. Since the inversion process required to extract droplet spectra from optical data involves significant uncertainty, they adopted the simple expedient of computing the light transmittances from the computed spectra and comparing directly with the measurements. Respectable agreement was obtained, but only by tuning of the assumed pitch-wise loss profiles.

Despite the success of the statistical wake-chopping model in predicting the correct qualitative behaviour, it is unlikely at this stage that such a technique could be employed for useful quantitative calculations. This is in part due to the requirement for tuning of loss parameters, but also because certain potentially important effects cannot easily be included within the model. Examples include: (i) pitch-wise variations in the expansion rate ($\dot{p} = -d \ln(p)/dt$) which is known to strongly influence the number of droplets nucleated [7]; (ii) interactions between blade trailing-edge shockwaves and the condensation zone which may serve to prematurely terminate the nucleation process [8]; (iii) the possible occurrence of condensation induced shockwaves due to supercritical heat release, such as those observed in nozzles [9]. Such phenomena (which may or may not have a bearing on the droplet spectra in real turbines) can only really be modelled by undertaking calculations of the complete flowfield, including full two-way coupling of the phase change.

Computational methods for fluid flow have now reached a stage whereby full unsteady, 3D viscous calculations are feasible for a complete multistage turbine. Furthermore, steam condensation effects can be incorporated into such methods with a relatively modest increase in computational requirement by adopting efficient look-up tables for steam properties, and by using the first few moments of the size distribution to represent the complete droplet spectrum. It is therefore timely to use such an approach to assess the impact of the wake chopping effect and other forms of unsteadiness. The method described herein is being developed to perform full 3D calculations but this paper details only preliminary 2D and quasi-3D results in order to demonstrate the concept.

2 THE NUMERICAL METHOD

The two phase wet steam mixture is assumed to comprise a fog of spherical liquid droplets dispersed throughout the continuous vapour phase. Fog droplets are sufficiently small that velocity slip between the phases may be assumed negligible. (Note that some slip must occur in real turbines, at least at the level of turbulent eddies, since substantial deposition onto blades is observed. However, the objective here is chiefly to compute the fog droplet size distribution and the inclusion of slip is an unwarranted complication for this purpose.) With the no-slip assumption, the conservation equations for the mixture as a whole are

identical to their single-phase counterparts, provided the density, ρ , specific enthalpy, h , and specific internal energy, e , are treated as mixture quantities, as discussed further below. The condensing flow solver employed for the present work has thus been developed by extension of a single-phase method, TBLOCK, which is a Reynolds-averaged Navier-Stokes solver developed by Denton. This code is based on Denton's other 3D flow solvers developed for turbomachinery applications [10, 11], but is more versatile (by virtue of the multi-block grid structure) and can perform efficient unsteady calculations by using implicit dual time-stepping [12]. The algorithm used for steady calculations and the inner steps of unsteady calculations is the explicit "scree" scheme [11] with spatially varied time steps. Turbulence is modelled with a simple mixing length approach combined with a slip condition at solid boundaries. Shear stresses at the boundaries are then computed from wall functions [10].

2.1 Modelling the Liquid Phase

Due to capillary effects, the droplet temperature, T_d , (and hence other liquid phase properties) is a function of droplet size. Furthermore, as described in Ref. [13], the specific internal energy of droplets comprises bulk and surface terms, the latter being a function of their size. This means that the liquid phase contribution to mixture specific properties (h, e etc.) should strictly be evaluated by integrating over the size distribution. However, experience has shown that very little error is incurred by evaluating liquid properties at the saturation temperature $T_s(p)$. This is so because T_d only differs significantly from T_s in the case of extremely small droplets which make only a small contribution to mixture quantities. (A similar argument applies for surface energy terms.) Thus, to a very good approximation, the mixture specific enthalpy is given by:

$$h = (1 - y)h_g + yh_\ell, \quad (1)$$

where h_g is the vapour phase specific enthalpy (evaluated at p and T_g), h_ℓ is the liquid specific enthalpy (evaluated at p and $T_s(p)$) and y is the wetness fraction which is determined by integrating the nucleation and droplet growth equations. Other mixture specific quantities are computed using expressions similar to Eqn. (1), and it is through relationships of this sort that the gas dynamic and condensation equations are linked.

Nucleation and growth occur over a range of vapour-phase conditions resulting in a polydispersion of droplet sizes. This is modelled here by computing the evolution of the first few moments of the droplet size distribution. This method was first introduced by Hill [14] and a detailed description of its derivation and the approximations involved may be found in Ref. [15]. For wet steam applications it is known that the moment method begins to incur sizeable errors once the droplet spectrum becomes very broad [16]. However, it is anticipated that the broad size

distributions measured in turbines stem from time-averaging of fluctuating spectra, rather than from there being a wide polydispersion of droplets at a fixed point in space and time. The moment approach should therefore remain valid. (Use of the so-called quadrature moment method [17] may also be able to improve the accuracy for broad distributions but requires additional computational effort and has not been implemented at this stage.)

The j^{th} moment of the droplet size distribution μ_j is defined by:

$$\mu_j = \int_0^\infty r^j f dr, \quad (2)$$

where r is the droplet radius and f is the droplet number density function so that $f dr$ is the number of droplets per unit mass of mixture in the size range r to $r + dr$. Low order moments have an obvious physical significance, with μ_0 , μ_2 and μ_3 being proportional to the number of droplets, total droplet surface area and total droplet volume respectively (all per unit mass of mixture). The wetness fraction is also related to the third moment through:

$$y = \frac{4}{3}\pi\rho_\ell\mu_3 \quad (3)$$

where ρ_ℓ is the liquid density.

As shown in Ref. [15], the evolution of the j^{th} moment is given approximately by:

$$\frac{\partial}{\partial t}(\rho\mu_j) + \nabla \cdot (\rho\mu_j\mathbf{u}) = j\rho\bar{G}\mu_{j-1} + \rho J r_*^j, \quad j = 0, 1, 2, 3 \quad (4)$$

where \bar{G} is a representative average growth rate (evaluated here at the surface-averaged droplet radius, $r_{20} = \sqrt{\mu_2/\mu_0}$), J is the nucleation rate and r_* is the critical radius. Other symbols are as defined in the nomenclature. Inspection of Eqn. (4) reveals that the evolution of μ_3 (and hence y) depends on μ_2 which in turn depends on μ_1 etc. Thus four additional conservation equations must be solved to compute the wetness fraction.

Nucleation A comprehensive review of nucleation rate expressions and their application to wet steam flows is given in Ref. [18]. For the results presented here, the classical rate equation has been used, combined with a correction for non-isothermal effects:

$$J = \frac{1}{1 + \phi} q_c \frac{\rho_g^2}{\rho\rho_\ell} \sqrt{\frac{2\sigma}{\pi m^3}} \exp\left(-\frac{4\pi r_*^2 \sigma}{3kT_g}\right) \quad (5)$$

where q_c is the condensation coefficient (assumed to be unity), m is the mass of a molecule, k is Boltzmann's constant, r_* is the

Kelvin-Helmholtz critical radius, σ is the surface tension (assumed to be the flat film value) and $(1 + \phi)$ is the non-isothermal correction factor. The definitions of r_* and ϕ are standard and may be found with discussion in Refs. [19, 20].

Droplet Growth Droplet growth is computed from Young's modified form of Gyarmathy's growth law:

$$G = \frac{dr}{dt} = \frac{\lambda (1 - r_*/r) (T_s(p) - T_g)}{h_{fg} \rho_l r (1 + 3.78 (1 - \nu) Kn / Pr)} \quad (6)$$

where λ is the thermal conductivity of the vapour, Pr is the vapour Prandtl number and Kn is the Knudsen number. The term $(1 - \nu)$ was proposed by Young [19] to improve agreement with low pressure nozzle experiments. The form of ν and discussion of its justification may be found in Refs. [19, 21] but it should be noted that the effect of this parameter is not dramatic. For the present calculations, $\nu \approx 0.5$.

2.2 Artificial Dissipation

Artificial dissipation is required to stabilise the numerical scheme and prevent short wavelength oscillations in the neighbourhood of discontinuities. Following Jameson [22], a blend of fourth and second order smoothing is employed, using a pressure-based switch to turn on the second order terms (and reduce the fourth order ones) near shockwaves. In addition, since nucleation results in very rapid increases in droplet number, a similar switch based on μ_3 is used to control smoothing terms for the moment conservation equations.

2.3 Steam Properties

Steam (vapour phase) properties have been included using a tabular Taylor series expansion method described in Ref. [23]. Properties and their first and second derivatives (with respect to internal energy and density) are stored in a look-up table and intermediate values are determined by interpolation. Any equation of state can in principle be used to generate the tables; that used here is described in Ref. [20] and is valid for pressures below 5 bar.

3 NOZZLE AND CASCADE CALCULATIONS

For the purposes of code validation, a number of nozzle and cascade condensing flows have been computed. A selection of these is presented here alongside experimental data where available.

3.1 Steady Nozzle Flow

Figure 1 shows the computed centre-line pressure distribution and Sauter mean droplet radius ($r_{32} = \mu_3 / \mu_2$) compared with

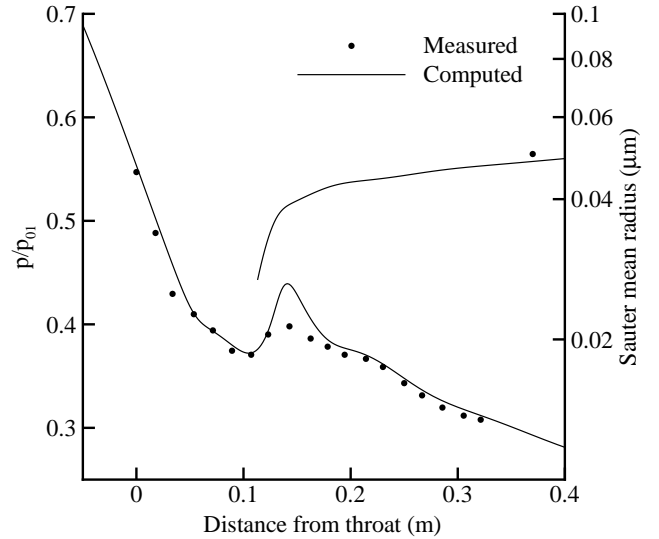


FIGURE 1. COMPARISON OF COMPUTED AND MEASURED CENTRE-LINE PRESSURE AND DROPLET RADIUS FOR NOZZLE B FROM [24]. INLET CONDITIONS: $P_{01} = 0.25$ BAR, $T_{01} = 358$ K.

experimental results for nozzle B of Moore *et al* [24]. The results shown have been computed with a structured 2D grid comprising 149×32 cells, which is sufficient for grid independence. The grid was stretched so that there was a high resolution in the region of nucleation and at the walls to resolve the boundary layers. (Coarse grids tend to smooth out temperature variations within the condensation zone, leading to the nucleation of fewer droplets which consequently grow to larger diameters.)

As discussed in Ref. [25], the discontinuity in curvature of the wall profile for nozzle B (and the other nozzles presented in [24]) leads to strong 2D effects which show up as undulations in the centre-line pressure. To some extent these are smoothed out by viscous effects, and consequently the computed results are sensitive to the assumed state of the boundary layer. In keeping with the findings presented in Ref. [25], best agreement with experiment is obtained for a turbulent boundary layer calculation. In the results shown the boundary layer grows from zero thickness at entry to the computational domain at $x = -0.22$ m. (Paradoxically, seemingly better agreement with the measured pressure distribution was obtained in Ref. [20] using a much coarser grid and an inviscid calculation method, but those results did not exhibit the pressure undulations discussed above. For further discussion, see Ref. [21].)

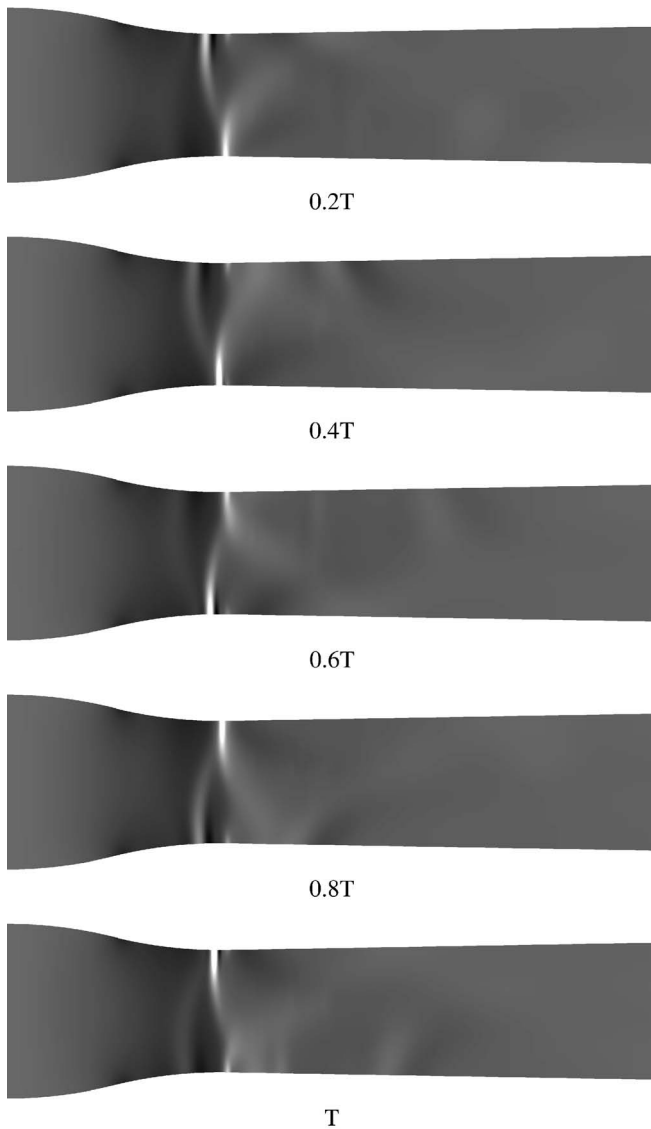


FIGURE 2. ASYMMETRIC SUPERCRITICAL OSCILLATIONS – NUMERICAL SCHLIEREN IMAGE (CONTOURS OF $\partial\rho/\partial x$) FOR NOZZLE E IN [24] WITH $P_{01} = 1$ BAR AND $T_{01} = 378$ K. (T IS THE PERIOD OF ONE OSCILLATION.)

3.2 Asymmetric Supercritical Oscillations

To demonstrate the unsteady capability of the code, calculations have been undertaken for so-called supercritical heat addition – i.e., where the latent heat release is more than sufficient to return the flow to sonic conditions. A particularly interesting example of this is the asymmetric oscillation phenomenon discovered by Adam & Schnerr [26] for moist air nozzle flows. Such oscillations were first observed experimentally but have also been simulated with inviscid flow calculations for both moist

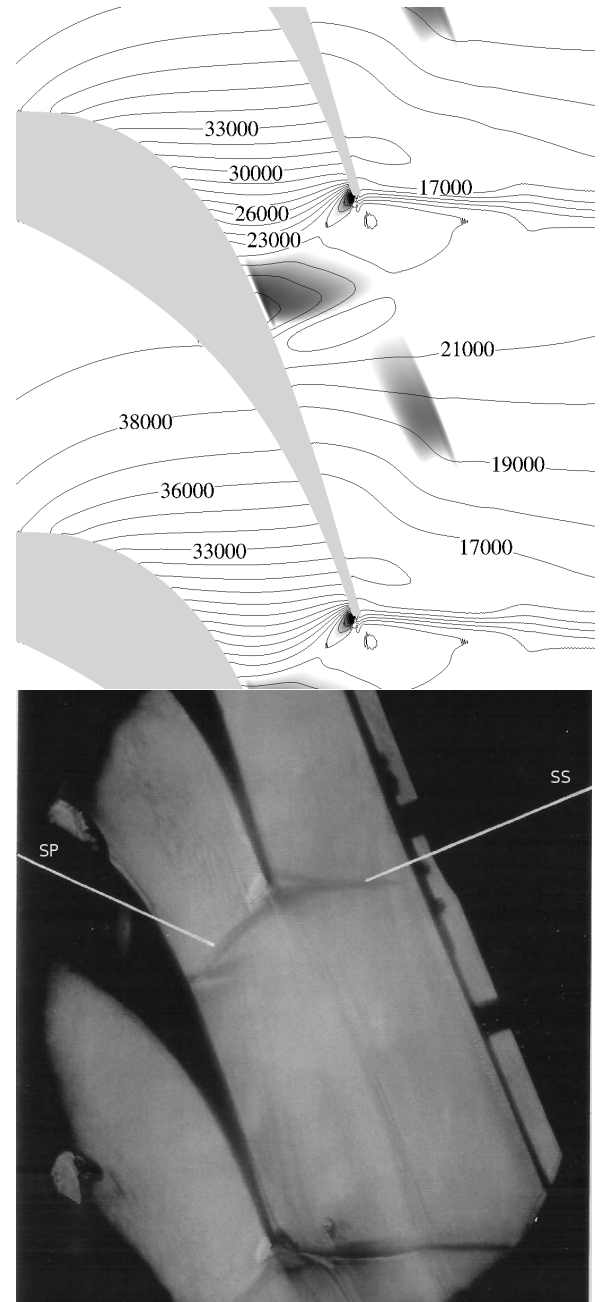


FIGURE 3. ABOVE: COMPUTED PRESSURE CONTOURS (Nm^{-2}) AND NUCLEATION RATE (SHADED); BELOW: SCHLIEREN IMAGE FOR TEST L2 IN [8]. $P_{01} = 0.409$ BAR, $T_{01} = 354$ K, ISENTROPIC EXIT MACH No. $M_{2s} = 1.11$. THE FEATURES CORRESPONDING TO THE SUCTION AND PRESSURE SURFACE SHOCKWAVES ARE LABELLED SS AND SP RESPECTIVELY.

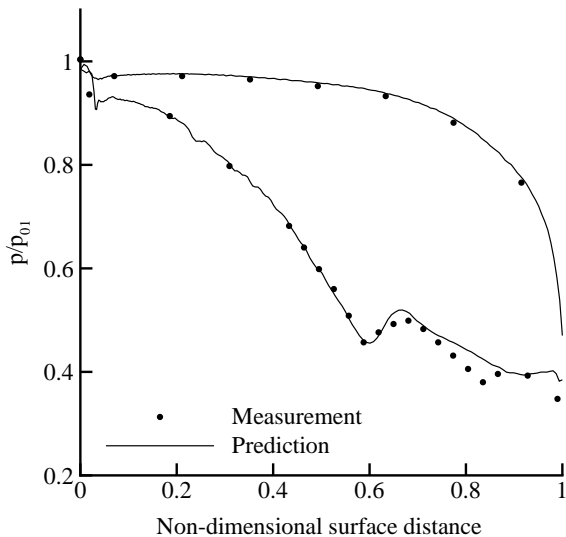


FIGURE 4. COMPUTED AND MEASURED BLADE SURFACE PRESSURE DISTRIBUTIONS FOR TEST L2 [8].

air [26] and pure steam [25]. Figure 2 shows computed shaded contours of $\partial\rho/\partial x$ (equivalent to a schlieren image) at five time intervals over a single period. This mode of oscillation comprises a complex sequence of unsteady, oblique shockwaves which interact with the condensation zone. Although there are no experimental data for this phenomena occurring in pure steam, the results shown in Fig. 2 bear very close resemblance to the sequence of oblique shock structures observed in the experiments of Adam & Schnerr for moist air.

It is conceivable that oscillatory behaviour of the sort described above may occur within turbine blade passages. As yet there is no evidence for this but, were it to be the case, it may have implications for aerodynamic performance and unsteady blade loading. Furthermore, periodic quenching of the nucleation process by the unsteady shockwaves is likely to result in broader size distributions with a larger average size, as shown in Ref. [21] for the case of symmetric oscillations.

3.3 Comparison with Cascade Experiments

As a final validation case, condensing flow in a cascade of LP turbine stator blades has been computed and the results compared with the experiments of White *et al* [8]. Due to space constraints, only one case is presented: that of test L2, conducted at a low inlet superheat and moderate exit Mach number. Computed pressure contours are shown in Fig. 3 alongside the experimental schlieren image. Figure 3 also shows regions of high nucleation rate (dark shading) which coincide with the feature emanating

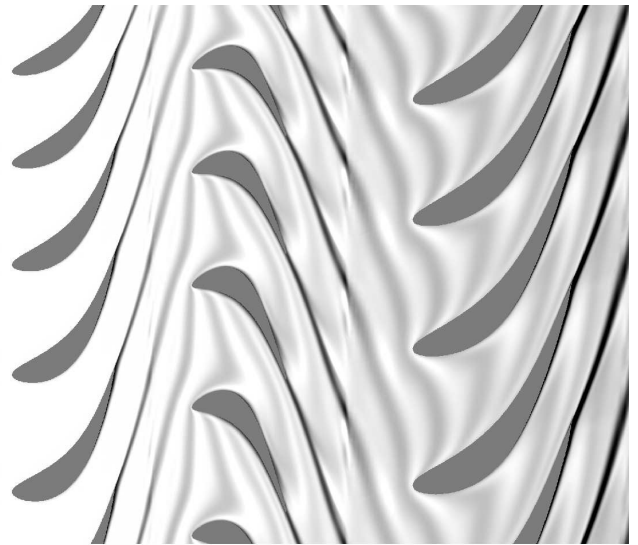


FIGURE 5. COMPUTED CONTOURS OF $\exp(-\Delta_s/R)$ FOR A TWO STAGE UNSTEADY QUASI-3D CALCULATION (DRY, PERFECT GAS FLOW).

from the suction surface of the blade in the schlieren image. As with other attempts at computing this case (e.g., Refs. [8, 27]), the pressure surface shockwave is found to interact with the nucleation zone such that significant condensation does not appear until further downstream over part of the pitch. It is clear that this sort of interaction will be sensitive to small numerical errors, highlighting the difficulties associated with predicting all the phenomena occurring within the turbine environment. Nonetheless, acceptable agreement between the computed and measured blade surface pressures is obtained, as shown in Fig. 4.

4 UNSTEADY QUASI-3D CALCULATIONS FOR A TWO STAGE LP TURBINE

An initial investigation of the wake-chopping effect is presented here, based on quasi-3D calculations for two consecutive LP turbine stages. The geometry is not that of a real turbine but is nonetheless intended to be representative of a $\sim 50\%$ reaction machine at mid span. Each blade row has the same number of blades which, although not realistic, means that only one passage per row needs to be computed. In order to assess the impact of wake-chopping, fully unsteady and steady calculations have been undertaken for comparison. For the latter, all flow variables are circumferentially averaged at the slip planes located roughly midway between the trailing edges of one blade row and the leading edges of the next.

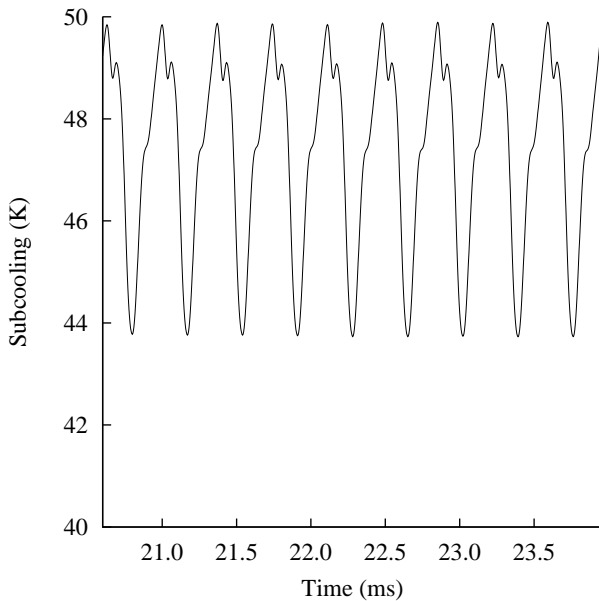


FIGURE 6. COMPUTED FLUCTUATION IN VAPOUR SUBCOOLING ($\Delta T = T_s - T_g$) AT A POINT (FIXED IN ROTOR FRAME OF REFERENCE) LOCATED MID PASSAGE NEAR THE FINAL ROTOR TRAILING EDGE (DRY, PERFECT GAS FLOW).

4.1 Dry Flow Calculations

Figure 5 shows shaded contours of dissipation in the form of $\exp(-\Delta s/R)$, where Δs is the difference between the local specific entropy and that at inlet to the flow domain. The results presented here are for a dry, perfect gas calculation (the steam is allowed to become super-saturated, but no condensation modeling is used) so that the wakes can be easily discerned (the condensation process engenders its own entropy increase which would obscure the wakes). Some smearing of the wakes occurs across the slip planes due to a discontinuity of the grid density – the upstream grid being refined in the vicinity of the wakes and the downstream grid being uniform – but wake segmentation in the successive blade rows is clearly visible in the figure, and it is evident that the core flow in each blade passage (i.e., outside of the boundary layers and where condensation is likely to be initiated) experiences fluctuating levels of dissipation. The impact that this is likely to have on the condensation process may be assessed by examining the resulting fluctuations in vapour subcooling ($\Delta T = T_s - T_g$), shown in Fig. 6 for a point located at mid passage and near the exit of the final rotor. The subcooling computed at this point in the steady calculation was 47.5 °C. The high values of subcooling shown here (above ~ 40 °C) are a consequence of this being a perfect gas calculation – in practice the latent heat release from condensation would increase the vapour temperature such that maximum values of ΔT would not

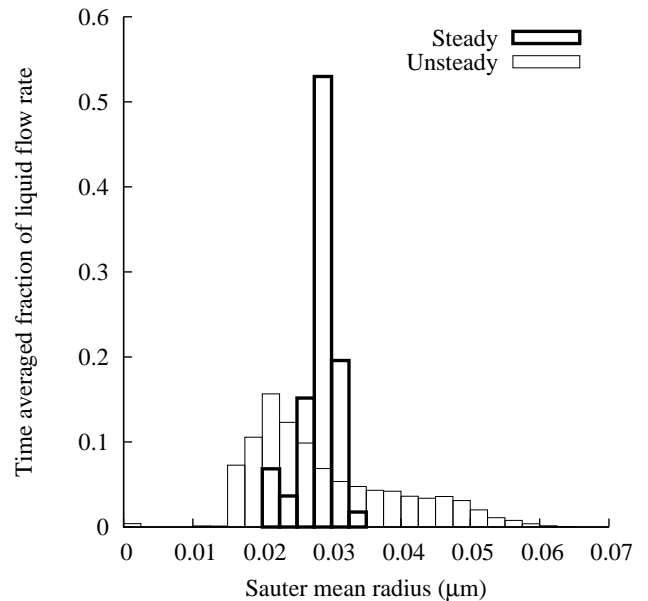


FIGURE 7. COMPUTED TIME-AVERAGED DROPLET SIZE DISTRIBUTIONS DOWNSTREAM OF THE SECOND ROTOR FOR STEADY (BOLD) AND UNSTEADY CALCULATIONS.

exceed 35 – 40 °C. Nonetheless, Fig. 6 serves to demonstrate that dramatically fluctuating nucleation rates are likely to result from the wake-induced unsteadiness. In this respect, it is worth noting that, at typical nucleating conditions, a 1 °C increase in ΔT will increase J by a factor of 2 – 3.

4.2 Condensing Flow Calculations

The two stage steady and unsteady calculations discussed above were repeated for condensing flow. Figure 7 shows the final, time-averaged distribution of droplet sizes as would be seen by a probe situated downstream of the final rotor. (Note that, since the moment method has been employed, only a single droplet radius, $r_{32} = \mu_3/\mu_2$, is computed at each point in time, but the averaging process results in a spectrum of sizes.) For the calculations presented, nucleation mainly commenced at the trailing edge of the final rotor. The expansion rate here at mid passage is approximately 3000 s^{-1} . The different sizes observed for the steady calculation thus stem from pitch-wise variations in the rotor passage, especially of the expansion rate, \dot{p} , and of the entropy increase due to viscous effects. The unsteady calculations clearly yield a much broader spectrum of sizes due to fluctuations in subcooling similar to those shown in Fig. 6. This result is in accord with the wake-chopping models discussed in section 1, but it is notable that the droplets are much smaller than those measured in real turbines, which typically have a mean diameter of 0.2 – 0.6 μm . However, the results presented here

represent only the first to emerge from this unsteady calculation method and further investigation is clearly required.

CONCLUDING REMARKS

A method for computing unsteady, viscous wet steam flows has been presented in outline. Results have been shown for nozzle and cascade test cases and show very good agreement with experimental data. The unsteady capability of the code has also been demonstrated by computing asymmetric, supercritical oscillations in nozzles, similar to those observed for moist air flow.

Application of the method to a two stage LP steam turbine shows how unsteadiness generated by upstream blade rows leads to fluctuating levels of subcooling in the final rotor, which in turn generates a spectrum of droplet sizes that is much broader than that obtained from steady calculations. Average droplet sizes predicted so far are smaller than observed in real turbines, but further calculations are needed to investigate all the potential effects; for example, it is likely that, had the calculations been extended to include additional downstream blade rows, further nucleation would be predicted as the hot wake flows from the second rotor continue to expand. Early indications, however, confirm the importance of wake-chopping in influencing fog formation.

ACKNOWLEDGMENT

The first author, KDC, is grateful for the support of the Engineering and Physical Sciences Research Council (EPSRC). All authors also wish to acknowledge the generous support from Alstom Power (Steam Turbines Division).

REFERENCES

- [1] Wróblewski, W., Dykas, S., and Gepert, A., 2009. "Steam Condensing Flow Modeling in Turbine Channels". *Int. J. Multiphase Flow*, **35**(6), pp. 498–506.
- [2] Gyarmathy, G., and Spengler, P., 1974. "Flow fluctuations in multistage thermal turbomachinery". In *Traupel-Festschrift, Juris-Verlag, Juris-Verlag*, pp. 95–141. (CEGB Translation 17551).
- [3] Bakhtar, F., and Heaton, A., 1988. "An examination of the effect of 'wake chopping' on droplet sizes in turbines". In *Conference on Technology of Turbine Plant Operating with Wet Steam*, BNES, pp. 197–200. London.
- [4] Guha, A., and Young, J. B., 1994. "The effect of flow unsteadiness on the homogeneous nucleation of water droplets in steam turbines". *Phil. Trans. R. Soc., Series A*, **349**, pp. 445–472.
- [5] Walters, P., 1988. "Improving the accuracy of wetness measurements in generating turbines using a new procedure for analysing optical transmission data". In *Conference on Technology of Turbine Plant Operating with Wet Steam*, BNES, pp. 207–215. London.
- [6] Petr, V., and Kolovratnik, M., 2000. "Modelling of the droplet size distribution in a low-pressure steam turbine". *Proc. Instn. Mech. Engrs*, **214**, pp. 145–152. Part A.
- [7] Huang, L. X., and Young, J. B., 1996. "An analytical solution for the wilson point in homogeneously nucleating flows". *Proc. R. Soc., Series A*, **452**, pp. 1459–1473.
- [8] White, A. J., Young, J. B., and Walters, P. T., 1996. "Experimental validation of condensing flow theory for a stationary cascade of steam turbine blades". *Phil. Trans. R. Soc., Series A*, **354**, pp. 59–88.
- [9] Skillings, S. A., Moore, M. J., Walters, P. T., and Jackson, R., 1988. "A reconsideration of wetness loss in lp steam turbines". In *Technology of Turbine Plant Operating with Wet Steam*, BNES, pp. 171–177.
- [10] Denton, J. D., 1992. "The calculation of 3-dimensional viscous-flow through multistage turbomachines". *Trans. ASME, J. Turbomachinery*, **114**, pp. 18–26.
- [11] Pullan, G., and Denton, J. D., 2003. "Numerical simulations of vortex-turbine blade interaction". In *Proceedings of the 5th European Conference on Turbomachinery*, Prague, pp. 1049 – 1059.
- [12] Jameson, A., 1991. "Time dependent calculations using multigrid, with applications to unsteady flows past airfoils and wings". In *AIAA 10th Computational Fluid Dynamics Conference*. Paper No. 91-1596.
- [13] Young, J. B., 1995. "The fundamental equations of gas-droplet multiphase flow". *Int. J. Multiphase Flow*, **21**(2), pp. 175–191.
- [14] Hill, P. G., 1966. "Condensation of water vapour during supersonic expansion in nozzles". *J. Fluid Mechanics*, **25**(3), pp. 593–620.
- [15] White, A. J., and Hounslow, M. J., 2000. "Modelling droplet size distributions in polydispersed wet-steam flows". *Int. J. Heat and Mass Trans.*, **43**(11), pp. 1873–1884.
- [16] White, A. J., 2003. "A comparison of modelling methods for polydispersed wet-steam flow". *Int. J. for Numer. Meth. Engng*, **57**(6), pp. 819–834.
- [17] Gerber, A. G., and Mousavi, A., 2007. "Representing Polydispersed Droplet Behaviour in Nucleating Steam Flow". *Trans. ASME, J. Fluids Eng.*, **129**, pp. 1404–1414.
- [18] Bakhtar, F., Young, J. B., White, A. J., and Simpson, D. A., 2005. "Classical nucleation theory and its application to condensing steam flow calculations". *Proc. Instn Mech. Engrs, Part C: J. Mech. Eng. Sci.*, **219**(12), pp. 1315–1333.
- [19] Young, J. B., 1982. "The spontaneous condensation of steam in supersonic nozzles". *Physicochemical hydrodynamics*, **3**(1), pp. 57–82.
- [20] Young, J. B., 1992. "Two-dimensional, nonequilibrium, wet-steam calculations for nozzles and turbine cascades".

Trans. ASME, J. Turbomachinery, **114**(3), pp. 569–579.

- [21] White, A. J., and Young, J. B., 1993. “Time-marching method for the prediction of two-dimensional, unsteady flows of condensing steam”. *J. Propulsion and Power*, **9**(4), pp. 579–587.
- [22] Jameson, A., Schmidt, W., and Turkel, E., 1981. “Numerical solution of the Euler equations by finite volume methods using Runge-Kutta time stepping schemes”. In AIAA 14th Fluids and Plasma Dynamics Conference. Paper No. 81-1259.
- [23] Hill, P. G., Miyagawa, K., and Denton, J. D., 2000. “Fast and accurate inclusion of steam properties in two- and three-dimensional steam turbine flow calculations”. *Proc. Instn Mech. Engrs, Part C: J. Mech. Eng. Sci.*, **214**(7), pp. 903–919.
- [24] Moore, M., Walters, P., Crane, R., and Davidson, B., 1973. “Predicting the fog-drop size in wet-steam turbines”. In Instn. mech. eng. conf. pub. Heat and Fluid Flow in Steam and Gas Turbine Plant, warwick, pp. 101–109. C37/73.
- [25] Simpson, D. A., and White, A. J., 2005. “Viscous and unsteady flow calculations of condensing steam in nozzles”. *Int. J. Heat and Fluid Flow*, **26**(1), pp. 71–79.
- [26] Adam, S., and Schnerr, G. H., 1997. “Instabilities and bifurcation of non-equilibrium two-phase flows”. *J. Fluid Mech.*, **348**, pp. 1–28.
- [27] Gerber, A. G., 2006. “Inhomogeneous multiphase model for nonequilibrium phase transition and droplet dynamics”. *ASME 2nd Joint U.S.-European Fluids Engineering Summer Meeting*, pp. pp. 941–952. Paper No. FEDSM2006-98460.